Electron cross section set for CHF_3

W. Lowell Morgan[a)]
Kinema Research and Software, P.O. Box 1147, 236 N. Washington Street, Monument, Colorado 80132

Carl Winstead[b)] and Vincent McKoy[c)]
A. A. Noyes Laboratory of Chemical Physics, California Institute of Technology, Pasadena, California 91125

(Received 2 February 2001; accepted for publication 7 May 2001)

We describe the development of a consistent set of low-energy electron collision cross sections for trifluoromethane, CHF_3. First-principles calculations are used to obtain key elastic and inelastic cross sections. These are combined with literature values of the ionization cross section and with vibrational excitation cross sections obtained from the Born approximation to form a preliminary set, which is then adjusted to achieve consistency with measured swarm parameters. © *2001 American Institute of Physics.* [DOI: 10.1063/1.1382833]

I. INTRODUCTION

Electron collision processes are critical in determining plasma properties,[1] yet for most gases of interest the available low-energy electron collision data are fragmentary. Modelers are often forced to rely on mutually inconsistent results drawn from disparate sources and even, employing intuition and analogy, to guess at cross section values. The resulting cross section sets are, apart from any other weaknesses, frequently inconsistent with swarm measurements. On the other hand, attempts to develop cross section sets from swarm data alone are hampered by a nonuniqueness problem that renders the individual cross sections so obtained suspect.

A clearly preferable alternative is to obtain data of high quality for the most important collision processes and to develop from those data, via a suitable process of adjustment, a cross section set that is consistent with swarm measurements. Because there are few gases for which sufficient high-quality data may be obtained from the literature, realization of this approach requires the ability to generate relevant cross sections as needed, either through calculation or experiment, and thus implies a collaborative effort between researchers engaged in determining electron–molecule collision properties and researchers experienced in swarm analysis.

In this article, we describe a collaborative process to develop an electron cross section set for the plasma etchant trifluoromethane, CHF_3. Essential cross section data not available in the literature—in particular, the cross sections for (dissociative) electron-impact excitation processes—are calculated from first principles. The calculated cross sections are then combined with cross sections for other important processes obtained from the literature or, in the case of vibrational excitation, the Born approximation. The resulting preliminary cross section set is then systematically refined to bring the swarm parameters predicted from it into agreement with measured values.[2,3] We find that the required adjustments to the calculated cross sections are modest and within the expected range. Differences between our final cross section set and previous sets[4–6] are discussed.

II. CROSS SECTION CALCULATIONS

A. Computational method

Cross sections for elastic electron scattering by and electron-impact excitation of CHF_3 were computed using the Schwinger multichannel (SMC) method[7,8] as implemented for parallel computers.[9,10] Details of the method may be found in the references given. For the present purpose, it is sufficient to mention that the SMC method is a variational method for the scattering amplitude based on quantum-mechanical first principles, and that its implementation is well suited to studies of low-energy electron collisions with polyatomic molecular targets. In particular, use of parallel computers facilitates numerically intensive studies of larger polyatomic systems that would be difficult or impossible to carry out on single-processor computers.

Details of the present calculations on CHF_3 are as follows. All scattering calculations were carried out at a geometry optimized using the program system GAMESS,[11] employing second-order Möller–Plesset perturbation theory and the 6-31G(d) basis set internal to GAMESS. This geometry, which belongs to the C_{3v} point group, has a C–H distance of 1.088 Å, a C–F distance of 1.343 Å, and an F–C–F angle of 108.45°. For comparison, the experimental equilibrium geometry[12] has a C–H distance of 1.098 Å, a C–F distance of 1.332 Å, and an F–C–F angle of 108.8°. Elastic scattering was studied in the static-exchange approximation, that is, neglecting polarization of the molecular charge density by the projectile electron during the course of the collision. This approximation improves with increasing collision energy and is generally quite accurate at collision energies above roughly 10 eV, except in the presence of resonances (temporary anions). For polar molecules such as CHF_3, the static-exchange approximation may also work well at lower energies, because the dipole potential may mask the effects of the more rapidly decaying polarization interaction at large dis-

a)Electronic mail: morgan@kinema.com
b)Electronic mail: carl@schwinger.caltech.edu
c)Electronic mail: mckoy@its.caltech.edu

tances. More elaborate calculations on CHF_3 that do consider the polarization effects below 15 eV[13] have recently been carried out.

Our implementation of the SMC method employs Cartesian Gaussian basis functions to represent both bound and scattering orbitals. The basis set used in the elastic calculations was the ''triple zeta valence'' (TZV) set internal to GAMESS[11] together with a $1s1p3d$ set of supplementary diffuse and polarization functions on the C and F atoms, for which the default GAMESS exponents were used, and a $2p$ supplement on H, with exponents 1.4 and 0.4. The basis set used in the electron-impact excitation calculations comprised the ''triple zeta'' set of Schäfer *et al.*[14] for the C and F atoms, the Huzinaga–Dunning $(4s)/[3s]$ basis[15,16] for the H atom, and the following supplement: on C, two diffuse *s* functions (exponents 0.047 and 0.023), three diffuse *p* functions (exponents 0.042, 0.021, and 0.0105), and three *d* functions (exponents 0.8, 0.3, and 0.015); on F, one diffuse *s* function (exponent 0.036), one diffuse *p* function (exponent 0.029), and two *d* functions (exponents 0.90 and 0.015); and on H, a diffuse *s* function (exponent 0.036) and two *p* functions (exponents 1.4 and 0.4). This basis set was intended to permit a good representation of the relevant excited states, which are mostly Rydberg in character. All six Cartesian components of the *d* functions were retained. In total, there were 154 and 143 contracted Gaussians in the basis sets used, respectively, for the elastic and inelastic calculations.

In an independent-orbital picture, the ground state of CHF_3 has the electronic configuration $(1a_1)^2(1e)^4(2a_1)^2(3a_1)^2(2e)^4(4a_1)^2(5a_1)^2(3e)^4(4e)^4(5e)^4(1a_2)^2(6a_1)^2$. Our elastic calculations used the Hartree–Fock wave function having this configuration to describe the target molecule, with all remaining virtual orbitals employed in the description of the scattering electron. In our inelastic studies, we focused on low-lying states expected to contribute to electron-impact dissociation. The highest occupied orbital, $6a_1$, is primarily of C–H bonding character. The orbitals immediately below it, $4e$, $5e$, and $1a_2$, are lone-pair F $2p$ orbitals not involved in the bonding, while the orbitals with C–F bonding character are considerably more tightly bound. With a view to dissociative excitation, therefore, excitations out of the $6a_1$ orbital are of special interest. Accordingly, we considered the singlet and triplet states arising from promotion of an electron from $6a_1$ to $7a_1$ and from $6a_1$ to $6e$, that is, the $\tilde{a}\,^3A_1$, $\tilde{A}\,^1A_1$, $\tilde{b}\,^3E$, and $\tilde{B}\,^1E$ excited states of CHF_3. Each of these excited states was represented by a single electronic configuration consisting of the ground-state Hartree–Fock orbitals and a $7a_1$ or $6e$ triplet improved virtual orbital.[17] The computed excitation thresholds were 12.20, 13.19, 13.42, and 14.17 eV for the $^3A_1$, $^1A_1$, ^3E, and ^1E states, respectively. For comparison, Larrieu *et al.*,[18] using considerably more sophisticated wavefunctions (multireference singles-and-doubles configuration interaction), obtained 10.89 eV for the $\tilde{A}\,^1A_1$ threshold and 11.76 eV for the $\tilde{B}\,^1E$ threshold, while high-energy electron impact studies[19] showed a threshold at 10.92 eV assigned as $6a_1 \rightarrow 3s$ (i.e., $\tilde{A}\,^1A_1$) and one at 11.95 eV assigned as $6a_1 \rightarrow 3p$ (i.e., $\tilde{B}\,^1E$).

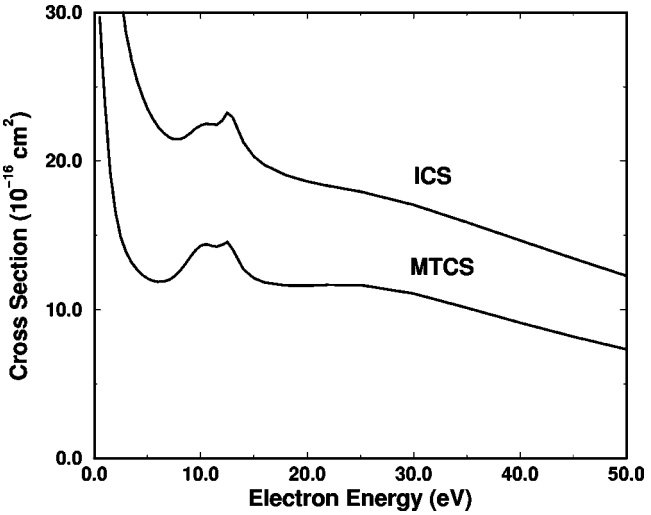

FIG. 1. Computed integral elastic cross section (ICS) and momentum transfer cross section (MTCS) for electron scattering by CHF_3.

Excitation cross sections were computed in a seven-channel, five-state approximation, coupling the elastic scattering channel to the $(6a_1 \rightarrow 7a_1)^{1,3}A_1$ and $(6a_1 \rightarrow 6e)^{1,3}E$ states. (The number of channels is greater than the number of states because the *E* states are doubly degenerate.) All unique configurations that could be formed by adding one of the virtual orbitals to one of the target configurations were employed in the variational space for the scattering wavefunction.

As a partial check on the elastic and excitation calculations just described, we also carried out calculations employing different basis sets and channel-coupling schemes. The static-exchange elastic cross sections obtained with a smaller basis set were very similar. Cross sections for the $\tilde{a}\,^3A_1$ and $\tilde{A}\,^1A_1$ states obtained from a three-channel calculation in a different basis set than the seven-channel results showed greater differences. The three- and seven-channel results for the $\tilde{A}\,^1A_1$ were qualitatively similar, but the peak value of the three-channel cross section was about a factor of 2 larger. For the $\tilde{a}\,^3A_1$ state, the peak value of the three-channel cross section was again larger, but the three-channel cross section fell well below the seven-channel result from about 19 to 28 eV. Two-channel results for the $\tilde{a}\,^3A_1$ state obtained in yet another basis set were qualitatively intermediate between the three- and seven-channel results. In all cases there was good agreement at higher energies. While the seven-channel results, arising from the most extensive coupling scheme considered, should in general be the most accurate, these comparisons do suggest that, at lower energies, the cross sections might change further upon inclusion of still more channels in the calculation.

B. Results and discussion

The integral elastic cross section (ICS) and momentum-transfer cross section (MTCS) calculated for CHF_3 are shown in Fig. 1. The sharp increase at the lowest energies shown is a common artifact of the static-exchange approximation. However, CHF_3 is a polar molecule, and long-range

scattering by the dipole potential, which is not fully included in our SMC cross sections because of the use of square-integrable basis sets, will lead to a *genuine* increase in the ICS and MTCS at these energies. We have included a correction for such long-range scattering using the Born completion procedure,[20,21] with partial-wave components of the scattering amplitude obtained from the SMC calculation used up to $l=5$, $m=4$ and the remainder of the scattering amplitude obtained from the first Born approximation for a point-dipole potential with strength 2.06 D; because this calculated value is considerably higher than the experimental value of 1.65 D,[22] and because of the artifactual increase of the static-exchange cross section, our low-energy cross section is probably overestimated. It should also be remarked that we have included a very small but finite inelasticity to avoid divergence of the Born cross section.

At higher energies, the static-exchange approximation becomes increasingly reliable. The main inaccuracies are probably in the location of the resonance features that give rise to the double hump in the calculated ICS and MTCS between 10 and 15 eV. With inclusion of polarization, such features typically move lower in energy by 1 to 4 eV. Experimentally, resonances were observed by Modelli *et al.* in electron transmission through CHF_3 at 6.3 and 9.3 eV.[23] Modelli *et al.* assigned the 9.3 eV feature to overlapping A_1 and E resonances but were unable to assign the 6.3 eV feature. Symmetry decomposition of the SMC cross section shows that the double-hump structure is due to overlapping E and A_1 resonances centered, respectively, at about 11 and 13 eV. Allowing for appropriate shifts in the resonance positions upon inclusion of polarization, our results confirm the assignment of the 9.3 eV feature by Modelli *et al.*, while leaving the origin of the 6.3 eV feature they observed unknown. Dissociative attachment experiments[24] showed peaks at 10.1 ± 0.1 and 12.3 ± 0.2 eV in the F^- production cross section, as well as a broad, weak peak centered at about 4.5 eV. Attachment peaks typically occur somewhat below the corresponding peaks in the elastic cross section, so the 4.5 eV peak may be associated with the feature seen in transmission at 6.3 eV. The 10.1 and 12.3 eV attachment peaks appear to correlate well with the computed positions of the E and A_1 resonances, but not with the 9.3 eV feature seen in the transmission spectrum. Further experimental study of the elastic and/or total cross section would be helpful in clarifying the situation.

Our computed elastic cross section is in generally good agreement with available experimental[13,25] and theoretical[13,26,27] results. The agreement is best judged by examining the differential cross sections, which are quite sensitive to computational limitations. Figure 2 shows a comparison of differential cross sections at various energies. As expected, the greatest discrepancies between the present results and both the experimental values and those obtained from the more elaborate calculations of Varella *et al.*[13] occur at low energies, due to omission of polarization effects in the present work.

Integral cross sections for electron-impact excitation of the $\tilde{a}\,^3A_1$, $\tilde{A}\,^1A_1$, $\tilde{b}\,^3E$, and $\tilde{B}\,^1E$ states obtained from the seven-channel calculation described earlier are shown in Fig. 3. Small oscillations in the cross sections are unlikely to be physical, but the broader peaks, centered at about 20 eV in the $\tilde{A}\,^1A_1$ cross section, 23 eV in the $\tilde{a}\,^3A_1$ and $\tilde{B}\,^1E$ cross sections, and 24 eV in the $\tilde{b}\,^3E$ cross section, may correspond to core-excited shape resonances. As expected, the cross sections for the optically forbidden triplet transitions fall off more rapidly at higher energies. In fact, the singlet cross sections are probably underestimated at the higher energies, because we have not included a correction for ''photonlike'' excitation in collisions at large impact parameters. However, the oscillator strengths of the $\tilde{A}$ and $\tilde{B}$ states are fairly small (0.036 and 0.023, respectively[18]), and the higher energies are less important in modeling of low-temperature plasmas, so omission of this correction is not expected to be material.

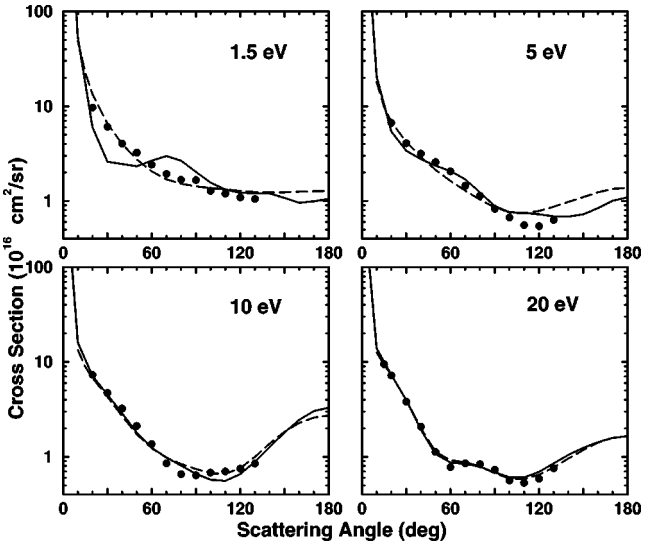

FIG. 2. Differential elastic electron scattering cross sections for CHF_3. Solid line: present result. Dashed line: calculation of Ref. 13. Circles: experimental values (Ref. 13).

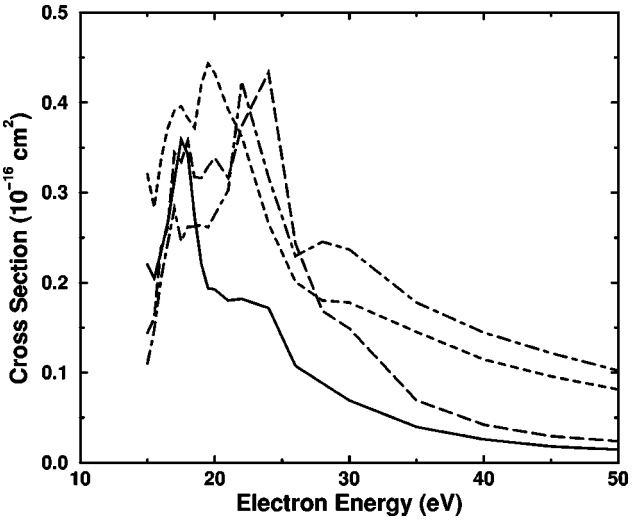

FIG. 3. Computed electron-impact excitation cross sections for four low-lying states of CHF_3. Solid line: $\tilde{a}\,^3A_1$ state. Short dashes: $\tilde{A}\,^1A_1$ state. Long dashes: $b\,^3E$ state. Dot-dashed line: $B\,^1E$ state.

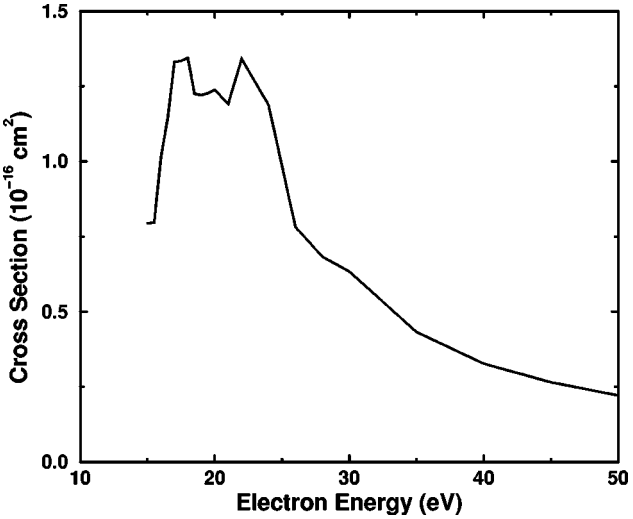

FIG. 4. Summed electron-impact excitation cross section for CHF_3.

The sum of the cross sections for the $\tilde{a}$, $\tilde{A}$, $\tilde{b}$, and $\tilde{B}$ states is shown in Fig. 4. (These data appeared also in a very preliminary account of the present work.[28]) This summed cross section will be used below to approximate the total electronic-excitation cross section of CHF_3. Although this is clearly a drastic approximation, a few points may be made in its favor. First, we have included the lowest-energy excitations; cross sections will in general decrease with increasing threshold. Also, as more channels are included in the channel-coupling scheme, the individual cross sections tend to decrease, at least at lower energies. Moreover, the calculations of Larrieu *et al.*[18] find no transitions with large oscillator strengths (which might be expected to have large electron cross sections also) below 15 eV, nor are there any intravalence transitions with low thresholds.

The vertical thresholds of all excited electronic states in CHF_3 lie well above the dissociation energy. Because the $\tilde{a}\,^3A_1$ state is the lowest triplet state, it is relatively easy to study by electronic-structure methods, and using a variety of approximations, we always found that its potential surface is repulsive along the C–H direction at the vertical geometry, with no barrier to dissociation. We therefore expect that almost all excitation to the $\tilde{a}$ state will result in fragmentation to CF_3+H. Dissociation behavior for the higher excited states is more difficult to study. However, we were able to gain some information by carrying complete-active-space self-consistent field (CASSCF) studies employing the program system MOLPRO.[29–31] In these studies, we considered each of the excited states successively, together with the ground state, in a state-averaged CASSCF calculation that preserved C_s symmetry and included eight active electrons in eight orbitals (six A' and two A''), and we carried out a geometry optimization for the excited state in small increments. These calculations indicated that the $\tilde{A}\,^1A_1$ state dissociates to CHF_2+F, while both the $\tilde{b}\,^3E$ state and the $\tilde{B}\,^1E$ dissociate to CHF+2F, in each case with no barrier to dissociation. Because of the restricted nature of these calculations, notably their imposition of C_s symmetry and omission of dynamics, these results should be considered suggestive rather than definitive, but they do indicate that none of the states considered is stable against dissociation and that F atoms may be produced.

III. SWARM ANALYSIS

A. Background

In an *electron swarm* measurement,[1,32] a burst of electrons is observed to drift along an electric field applied to a low-density gas, and various transport coefficients, such as the drift velocity, transverse or longitudinal diffusion coefficients, attachment or ionization coefficients, and so on are measured as functions of the applied electric field divided by the pressure or by the gas number density (i.e., E/p or E/N); collision cross sections, which are related to the transport coefficients through Boltzmann's transport equation, can be extracted by a process of inversion.

The current density is given by

$$\vec{j}_e = -eN_e\vec{v}_d = -\frac{1}{3}\left(\frac{2e}{m}\right)^{1/2}\frac{\vec{E}}{N_n}\int \frac{\mathrm{d}f_0(\varepsilon,E/N)}{\mathrm{d}\varepsilon}\frac{\varepsilon\,\mathrm{d}\varepsilon}{\sigma_m(\varepsilon)}, \tag{1}$$

where ε is the electron energy and $\vec{v}_d$ is the drift velocity. Since it is usually in the direction of the applied electric field, the drift velocity is often denoted as the scalar v_d. The quantity $f_0(\varepsilon)$ is the electron energy distribution function, while $\sigma_m(\varepsilon)$ is known as the *momentum-transfer cross section* and is defined by

$$\sigma_m(\varepsilon) = 2\pi\int \sigma_e(\varepsilon,\theta)(1-\cos\theta)\sin\theta\,\mathrm{d}\theta, \tag{2}$$

where $\sigma_e(\varepsilon,\theta)$ is the differential cross section for elastic scattering, θ being the scattering angle. The momentum transfer cross section is also known in transport theory as the diffusion cross section. For a uniform differential cross section, i.e., $\sigma_e(\varepsilon,\theta)$ constant as a function of θ, the elastic and momentum transfer cross sections are equal, i.e., $\sigma_m(\varepsilon) = \sigma_e(\varepsilon)$. When $\sigma_e(\varepsilon,\theta)$ is strongly peaked in the forward direction, then $\sigma_m(\varepsilon) < \sigma_e(\varepsilon)$, and when it is peaked in the backward direction, then $\sigma_m(\varepsilon) > \sigma_e(\varepsilon)$.

Derived quantities often seen in the plasma literature are the ionization and attachment coefficients $\alpha = k_i N_n/v_d$ and $\eta = k_a N_n/v_d$, which have units of cm^{-1} and represent the increase or decrease in electron density per centimeter due, respectively, to ionization and attachment. These quantities are directly measurable in a drift tube. The respective rate coefficients for ionization and attachment, k_i and k_a, are given in terms of the respective cross sections σ_i and σ_a by

$$k_{i,a} = \left(\frac{2e}{m}\right)^{1/2}\int \sigma_{i,a}(\varepsilon) f_0(\varepsilon)\varepsilon\,\mathrm{d}\varepsilon. \tag{3}$$

Most applications of swarm-derived cross sections in gas-discharge modeling use what amounts to an effective momentum transfer cross section, which is obtained by fitting to calculated and measured electron swarm data and may include sizable inelastic contributions. For this reason, the cross sections that are derived from swarm data may not agree with those separately measured in beam devices or computed using *ab initio* quantum techniques. The general

wisdom is that this approach works well because the cross sections are derived by fitting exactly the same coefficients, i.e., drift, diffusion, ionization, attachment, etc., that are used in fluid models of discharge plasmas. This leads to a self-consistency that has worked well over the years.

Modern high-vacuum beam measurement techniques and modern *ab initio* multichannel quantum calculations performed on supercomputers can provide very accurate cross sections for low-energy elastic and inelastic collisions. It often happens, however, that when the best data are assembled into a model for a molecule and transport calculations are performed, the agreement with measured transport (i.e., swarm) data is not very good. For example, we might assemble a detailed model using accurate cross sections from disparate sources and find that the computed ionization coefficient differs from that measured in a drift tube by an order of magnitude or more. If modeling plasma chemistry using very detailed and correct cross sections does not reproduce very accurately the plasma measurables in a well-defined and controlled swarm experiment, then the value of such modeling appears dubious.

Two reasons account for the disagreements between models based on cross sections and swarm measurements. First, the individual and independent errors (both in magnitude and energy dependence) in the separate cross sections from different sources may conspire to produce a sizable overall error. Second, including all known cross sections, or cross sections for all processes *believed* to be important, does not necessarily include all processes that *are* important. It is somewhat analogous to the missing matter problem in cosmology: all that we know may only be a fraction of what there is. This is where swarm analysis can make an important contribution. By their nature, swarm-derived cross sections include all processes either explicitly, as individual cross sections, or implicitly, contained within other cross sections. The latter possibility is another reason why swarm-derived cross sections often differ from those obtained by beam measurements or calculations.

We have used the following procedure for dealing with the potential problem of a collection of cross sections producing erroneous plasma transport coefficients:

(1) assemble the most complete models that we can using data from the sources discussed above;
(2) perform swarm calculations for conditions appropriate to transport measurements when such data are available;
(3) systematically renormalize and modify the energy dependence of the cross sections in order to reproduce the measured transport coefficients.

B. CHF_3 cross section set

One of the electron collision processes most important in plasma processing is neutral dissociation. If we have available *reliable ionization cross sections* and *swarm measurements* of both the drift velocity v_d and the ionization coefficient $\alpha(E/N)$, we can normalize computed dissociation cross sections or even derive approximate cross sections by means of swarm analysis. Because the ionization coefficient is an integral of the ionization cross section over the electron energy distribution function $f_0(\varepsilon,E/N)$, as shown earlier, for electron energies greater than the dissociation threshold and in certain ranges of E/N, $f_0(\varepsilon,E/N)$ is sensitive to the magnitude and energy dependence of the dissociation cross sections. This sensitivity is shown in Fig. 5, where we have plotted $f_0(\varepsilon,E/N)$ for three scaled values of the CHF_3 dissociation cross section. One can see how the high-energy tail of $f_0(\varepsilon,E/N)$ is affected, which in turn affects the value of $\alpha(E/N)$. We exploit this sensitivity to obtain information on the dissociation cross section.

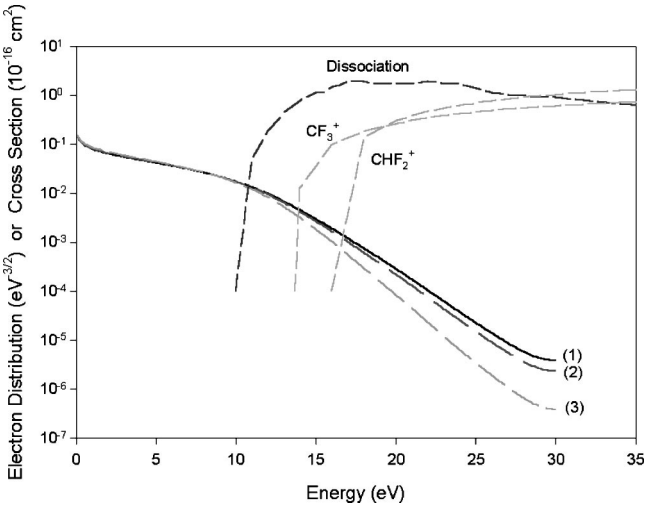

FIG. 5. Sensitivity of the electron energy distribution function to variations in the dissociation cross section: (1) $f_0(\varepsilon)$ at $E/N=200$ Td using the cross sections shown in Fig. 2; (2) $f_0(\varepsilon)$ with σ_d multiplied by 1.2; (3) $f_0(\varepsilon)$ with σ_d multiplied by 2.0.

Because our primary interest in assembling a cross section set for CHF_3 is in estimating the dissociation cross section, we are concerned mostly with cross sections at energies greater than several eV. For this reason, we use very approximate models for the vibrational cross sections in the absence of good molecular calculations or measurements. If $\Delta\varepsilon$ is the vibrational excitation energy in eV with ε the electron impact energy, then the cross section for excitation in the first Born approximation is[33]

$$\sigma_v^B=\frac{3.7\times10^{-15}}{\Delta\varepsilon x}\ln\left[\frac{x^{1/2}+(x-1)^{1/2}}{|x^{1/2}-(x-1)^{1/2}|}\right], \tag{4}$$

where $x=\varepsilon/\Delta\varepsilon$ and the normalization is such that the peak value of σ_v^B is $1\times10^{-16}\,\mathrm{cm}^2$. The vibrational excitation energies that we use for CHF_3 are 0.14 and 0.37 eV.

In order to estimate the dissociation cross section, we have constructed a cross section set comprising

(1) the computed momentum transfer cross section described earlier;
(2) two model vibrational cross sections;
(3) the computed dissociation cross section described earlier; and
(4) the measured partial ionization cross sections.[34]

Using this cross section set and the two-term spherical harmonic approximation,[35] we have solved Boltzmann's equa-

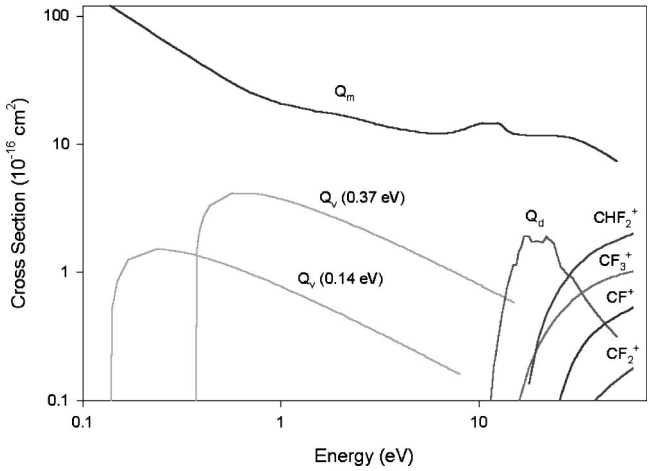

FIG. 6. CHF_3 cross section set optimized to be consistent with measured swarm data.

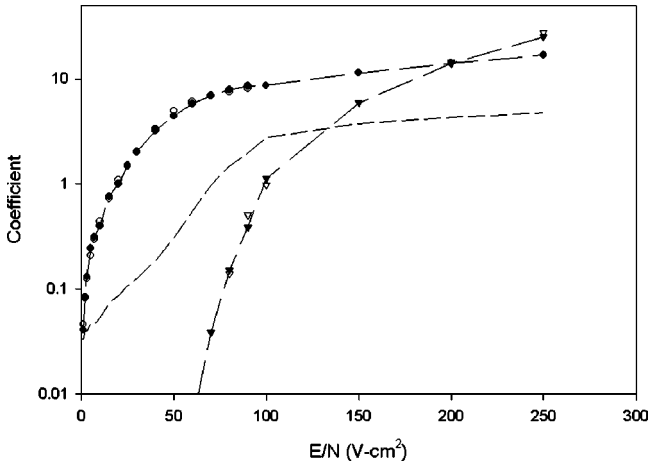

FIG. 7. Comparison of measured (solid symbols) and calculated (open symbols) drift velocity and ionization coefficient versus E/N. The calculated reduced mean energy is also shown.

tion for the electron energy distribution function $f_0(\varepsilon)$ as a function of E/N and computed the electron swarm coefficients.

In developing a self-consistent set of cross sections for CHF_3, we found that we were able to achieve good agreement between calculated and measured v_d and α by adjusting only the magnitudes of the momentum transfer cross section, the model vibrational excitation cross sections, and the dissociation cross section. The energy dependencies of the calculated $\sigma_m(\varepsilon)$ and $\sigma_d(\varepsilon)$ are accurate enough that we did not need to adjust the shapes of the cross sections.

There are a number of algorithms for varying the magnitudes of the cross sections in a systematic manner. We have used the downhill simplex algorithm,[36,37] which we have used previously[38,39] for varying both the magnitudes and the energy dependencies of cross sections. We vary scale factors that multiply the cross sections in order to minimize the function

$$\chi^2=\sum_i \left(\frac{v_d^c-v_d^m}{v_d^m}\right)^2+\left(\frac{\alpha^c-\alpha^m}{\alpha^m}\right)^2, \tag{5}$$

where the "c" and "m" superscripts denote calculated and measured values, respectively, and the sum is over all values of $(E/N)_i$. In our analysis, we have used the drift velocity measured by Wang *et al.*[2] and the ionization coefficient measured by de Urquijo *et al.*[3] Because Wang *et al.* found little or no dissociative attachment to CHF_3, we have ignored attachment in our swarm analysis.

The cross section set that we have derived for CHF_3, which is consistent with the swarm measurements, is shown in Fig. 6; numerical values are available at http://www.kinema.com on the World Wide Web. Following the swarm analysis procedure described earlier, the momentum transfer cross section remained within a few percent of that computed by *ab initio* methods. The dissociation cross section, however, required a multiplier of 1.4. The excellent agreement between swarm coefficients calculated using this cross section set and measurements is shown in Fig. 7. The computed rate coefficients for electron collision processes in CHF_3 are shown in Fig. 8. The rate coefficients shown in Fig. 8 have been fitted to the Arrhenius form,

$$k(T_e)=\alpha T_e^{\beta}\exp[-\gamma/T_e]\text{cm}^3/\text{s}, \tag{6}$$

with T_e in eV and for $0.5\,\text{eV}\leqslant T_e\leqslant 15\,\text{eV}$. The values obtained for α, β, and γ are shown in Table I.

A significant feature of this cross section set is that the dissociation cross section is much larger than that included in the cross section set of Christophorou *et al.*[4,5] from the measurements of Goto *et al.*[40] and of Sugai *et al.*[41] Both our own calculations and independent experiments[42,43] suggest that the dissociation cross sections reported by Sugai *et al.*[40,41] are in general too small, and indeed Christophorou and Olthoff[5] note this point. A similar conclusion was reached by Kushner and Zhang,[6] who, in developing a CHF_3 cross section set, first scaled the cross sections of Sugai *et al.* upward by a factor of 5, then added a further *ad hoc* near-threshold enhancement to improve the agreement with swarm data.

Of the previous publications of CHF_3 cross section sets,[4–6] the reviews of Christophorou *et al.*[4,5] presented exhaustive summaries of available collision data and even pro-

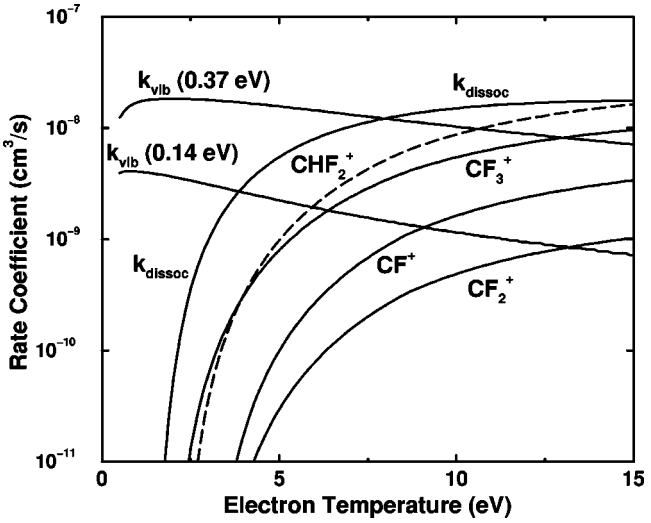

FIG. 8. Rate coefficients for electron collisions with CHF_3.

TABLE I. Rate coefficient parameters for use in Eq. (5).

Process (threshold)	α	β	γ
Vibration (0.14 eV)	9.225×10^{-9}	-8.724×10^{-1}	6.117×10^{-1}
Vibration (0.37 eV)	4.190×10^{-8}	-5.814×10^{-1}	7.352×10^{-1}
Dissociation (10.0 eV)	1.172×10^{-7}	-3.545×10^{-1}	$1.263\times10^{+1}$
Ionization (CHF_3^+, 13.72 eV)	1.033×10^{-8}	3.607×10^{-1}	$1.500\times10^{+1}$
Ionization (CHF_2^+, 13.82 eV)	1.845×10^{-8}	4.022×10^{-1}	$1.708\times10^{+1}$
Ionization (CF_2^+, 14.02 eV)	2.429×10^{-9}	2.566×10^{-1}	$2.233\times10^{+1}$
Ionization (CF^+, 16.94 eV)	1.190×10^{-8}	1.276×10^{-1}	$2.316\times10^{+1}$

vided a recommended cross section set. The authors did not, however, perform swarm calculations in order to check the consistency between their set of recommended cross sections and the electron transport measurements. Kushner and Zhang,[6] on the other hand, performed a swarm analysis similar to that reported here but with substantially different results. Their momentum transfer cross section is similar to ours but lacks the pronounced resonance structure around 10 eV. This is important because it affects the calculation of the drift velocity and, hence, the calculation of the ionization coefficient. There are profound differences between our composite neutral dissociation cross section and that presented by Kushner and Zhang. Our cross section has its peak value in the region between 17 and 22 eV, with a magnitude more than twice the values recommended by Kushner and Zhang, whereas the sum of their dissociation cross sections rises monotonically to about 100 eV. However, the swarm coefficients are only sensitive to features below approximately 20–25 eV, and the swarm analysis thus has nothing to say about the cross section at higher energies. We believe the differences between our results and those of Kushner and Zhang to be due to the following aspects of their work:

(1) use of different partial ionization cross section measurements having very different energy dependencies near threshold,
(2) use of total scattering cross section instead of a momentum-transfer cross section below 10 eV and of a coarse-grained *ab initio* momentum-transfer cross section above 10 eV, and
(3) simple scaling, by a large factor, of measured dissociation cross sections.

Regarding items (2) and (3), we believe that the *ab initio* momentum-transfer and dissociation cross sections that we have used produce a better starting point for the swarm calculations and, ultimately, a better outcome.

IV. SUMMARY

We have described the development of an electron collision cross section set for CHF_3 that is consistent with available swarm data. Key features of our work are the use of *ab initio* quantum-mechanical calculations to obtain important cross sections otherwise unavailable and the use of systematic procedures for adjusting all cross sections to obtain consistency with known swarm parameters. The resulting cross section set is expected to be of use in modeling of CHF_3 plasmas, and the approach followed in obtaining it is being applied to other gases of current interest.

ACKNOWLEDGMENTS

This research was supported by Sematech, Inc. Work at Caltech was also supported by the Office of Basic Energy Sciences of the Department of Energy and by an equipment grant from Intel Corp. Calculations reported here made use of the facilities of the Caltech Center for Advanced Computing Research and of the Jet Propulsion Laboratory's Supercomputing Project. The authors would like to thank Dr. Sadasivan Shankar of Intel Corp. for useful discussions and for his interest throughout the course of this work.

[1] W. L. Morgan, Adv. At., Mol., Opt. Phys. **43**, 155 (2000).
[2] Y. Wang, L. G. Christophorou, J. K. Olthoff, and J. K. Verbrugge, Chem. Phys. Lett. **304**, 303 (1999).
[3] J. de Urquijo, I. Alvarez, and C. Cisneros, Phys. Rev. E **60**, 4990 (1999).
[4] L. G. Christophorou, J. K. Olthoff, and M. V. V. S. Rao, J. Phys. Chem. Ref. Data **26**, 1 (1997).
[5] L. G. Christophorou and J. K. Olthoff, J. Phys. Chem. Ref. Data **28**, 967 (1999).
[6] M. J. Kushner and D. Zhang, J. Appl. Phys. **88**, 3231 (2000).
[7] K. Takatsuka and V. McKoy, Phys. Rev. A **24**, 2473 (1981).
[8] K. Takatsuka and V. McKoy, Phys. Rev. A **30**, 1734 (1984).
[9] C. Winstead and V. McKoy, Adv. At., Mol., Opt. Phys. **36**, 183 (1996).
[10] C. Winstead, C.-H. Lee, and V. McKoy, in *Industrial Strength Parallel Computing: Programming Massively Parallel Processing Systems*, edited by A. Koniges (Morgan-Kaufmann, San Francisco, 2000), p. 247.
[11] M. W. Schmidt *et al.*, J. Comput. Chem. **14**, 1347 (1993).
[12] S. N. Ghosh, R. Trambarulo, and W. Gordy, J. Chem. Phys. **20**, 605 (1992).
[13] M. T. do N. Varella, C. Winstead, V. McKoy, M. Kitajima, and H. Tanaka, Phys. Rev. A (submitted).
[14] A. Schäfer, C. Huber, and R. Ahlrichs, J. Chem. Phys. **100**, 5829 (1994).
[15] S. Huzinaga, J. Chem. Phys. **42**, 1293 (1965).
[16] T. H. Dunning, Jr., J. Chem. Phys. **53**, 2823 (1970).
[17] W. J. Hunt and W. A. Goddard, Chem. Phys. Lett. **3**, 414 (1969).
[18] C. Larrieu, M. Chaillet, and A. Dargelos, J. Chem. Phys. **94**, 1327 (1991).
[19] W. R. Harshbarger, M. B. Robin, and E. N. Lassettre, J. Electron Spectrosc. Relat. Phenom. **1**, 319 (1972).
[20] D. W. Norcross and N. T. Padial, Phys. Rev. A **25**, 226 (1982).
[21] T. N. Rescigno and B. I. Schneider, Phys. Rev. A **45**, 2894 (1992).
[22] W. L. Meerts and I. Ozier, J. Chem. Phys. **75**, 596 (1981).
[23] A. Modelli, F. Scagnolari, G. Distefano, D. Jones, and M. Guerra, J. Chem. Phys. **96**, 2061 (1992).
[24] H.-U. Scheunemann, M. Heni, E. Illenberger, and H. Baumgärtel, Ber. Bunsenges. Phys. Chem. **86**, 321 (1982).
[25] H. Tanaka, T. Masai, M. Kimura, T. Nishimura, and Y. Itikawa, Phys. Rev. A **56**, 3338 (1997).
[26] A. P. P. Natalense, M. H. F. Bettega, L. G. Ferreira, and M. A. P. Lima, Phys. Rev. A **59**, 879 (1999).
[27] R. B. Diniz, M. A. P. Lima, and F. J. da Paixão, J. Phys. B **32**, L539 (1999).

[28] V. McKoy, C. Winstead, and C.-H. Lee, J. Vac. Sci. Technol. A **16**, 324 (1998).
[29] MOLPRO is a system of *ab initio* programs written by H.-J. Werner and P. J. Knowles, with contributions from J. Almlöf, R. D. Amos, A. Berning, D. L. Cooper, M. J. O. Deegan, A. J. Dobbyn, P. Eckert, S. T. Elbert, C. Hampel, R. Lindh, A. W. Lloyd, W. Meyer, A. Nicklass, K. Peterson, R. Pitzer, A. J. Stone, P. R. Taylor, M. E. Mura, P. Pulay, M. Schütz, H. Stoll, and T. Thorsteinsson.
[30] H.-J. Werner and P. J. Knowles, J. Chem. Phys. **82**, 5053 (1985).
[31] P. J. Knowles and H.-J. Werner, Chem. Phys. Lett. **115**, 259 (1985).
[32] L. G. H. Huxley and R. W. Crompton, *The Diffusion and Drift of Electrons in Gases* (Wiley, New York, 1974).
[33] N. F. Lane, Rev. Mod. Phys. **52**, 29 (1980).
[34] C. Q. Jiao, R. Nagpal, and P. D. Haaland, Chem. Phys. Lett. **269**, 117 (1997).
[35] W. L. Morgan and B. M. Penetrante, Comput. Phys. Commun. **58**, 127 (1990).
[36] W. H. Press, S. A. Teukolsky, W. T. Vetterling, and B. P. Flannery, *Numerical Recipes in Fortran 77*, 2nd ed. (Cambridge U. P., New York, 1992).
[37] N. Gershenfeld, *The Nature of Mathematical Modeling* (Cambridge U. P., New York, 1999).
[38] W. L. Morgan, Phys. Rev. A **44**, 1677 (1991).
[39] W. L. Morgan, J. Phys. D **26**, 209 (1993).
[40] M. Goto, K. Nakamura, H. Toyoda, and H. Sugai, Jpn. J. Appl. Phys., Part 1 **33**, 3602 (1994).
[41] H. Sugai, H. Toyoda, T. Nakano, and M. Goto, Contrib. Plasma Phys. **35**, 415 (1995).
[42] L. Mi and R. A. Bonham, J. Chem. Phys. **108**, 1910 (1998).
[43] S. Motlagh and J. H. Moore, J. Chem. Phys. **109**, 432 (1998).